Bulletin of Geophysics and Oceanography Vol. XX, n. X, pp. XXX-XXX; Xxxxx 20xx
DOI 10.4430/bgo00463

Geophysical characterisation of asphalt pavement failure: a case study from the campus of South Valley University, Qena, Egypt

A.M. Abdelgowad[1], A.M. Ibrahim[1] and M.A. Abbas[1,2]

[1] *Geology department, Faculty of Science, South Valley University, Qena, Egypt*
[2] *Department of Earth, Environmental and Resources Sciences, University of Naples Federico II, Naples, Italy*

(Received: 21 December 2023; accepted: 20 May 2024; published online: 23 August 2024)

ABSTRACT Near-surface seismic refraction tomography and electrical resistivity imaging were used to study the collapse and subsidence of two asphalt roads on the campus of South Valley University in southern Egypt. The roads surround a garden where irrigation water was suspected to be the cause of the damage to the asphalt roads. Two seismic refraction tomography (SRT) lines were measured on the asphalt roads, and a single SRT line and an electric resistivity tomography (ERT) line were measured within the garden. The tomographic inversion of the SRT lines on the road shows several low velocity anomalies indicating areas of weakness beneath the asphalt. The SRT and ERT lines in the garden show a thin surface soil of fine sand and clay overlying a low electric resistivity and low seismic velocity clay layer. Examination of the results suggests that the damage to the asphalt roads could be caused by the presence of loose silt and clay soil that was used as a sub-base for the asphalt. This soil had not been compacted and engineered for use as a strong base layer. Instead, the asphalt was laid directly on top of it, which later led to the failure of the roads.

Key words: seismic refraction tomography, electrical resistivity imaging, asphalt pavement failure, velocity anomalies.

1. Introduction

Over the years, the use of geophysical techniques for civil engineering purposes has increased due to their reliable, repeatable, low-cost, and non-destructive nature. The continuous development of accurate, high-performance, and high-resolution techniques for data acquisition and processing, makes the near-surface geophysical methods such as seismic refraction tomography (SRT), multi-channel analysis of surface waves (MASW), ground penetrating radar (GPR), and electric resistivity tomography (ERT), prevailing techniques in detecting engineering problems.

The combined use of the seismic refraction method and the 2D geoelectrical method, is a fundamental tool for shallow target investigations related to civil engineering and applied geology applications (e.g. Whitlow, 1995; Abidin *et al.*, 2011). Both methods are used in subsoil and foundation evaluation (e.g. Cardarelli *et al.*, 2014; Butchibabu *et al.*, 2019), geotechnical site investigation (e.g. Yilmaz *et al.*, 2006; Azwin *et al.*, 2015; Fernández-Baniela *et al.*, 2021; Vagnon *et al.*, 2022a, 2022b; Qaher *et al.*, 2023) determining depth to bedrock and/or sedimentary cover

thickness (e.g. Zakaria *et al*., 2018; de Pasquale *et al.,* 2019), shallow subsurface and shallow structure investigation (e.g. Araffa *et al*., 2014, 2017; Villani *et al.*, 2015; Demirci *et al.*, 2017), and estimating depth to water table (e.g. Araffa *et al*., 2017, 2019; Aizebeokhai *et al.*, 2018). In addition, the application of electrical resistivity and seismic methods could help in identifying clay layers (Abidin *et al.*, 2012). The development of joint inversion approaches of both SRT and ERT data (e.g. De Nardis *et al.*, 2005; Gunther and Rucker, 2006; Garofalo *et al.*, 2015; Wagner *et al.*, 2019) improves the inversion results, increases the resolution, and reduces the inherent limitations of each method (Gallardo and Meju, 2003, 2004; Ronczka *et al.*, 2017; Imani *et al.*, 2021; Pavoni *et al.*, 2023).

In the present study, the site under investigation occupies a small area (about 1500 m^3) on the campus of South Valley University in Qena City, Egypt (Fig. 1). The site contains a newly constructed rectangular garden, 55 m long and 20 m wide. The grass in the garden is watered with the help of a sprinkler system. The garden is bordered to the north and south by two asphalt roads. The two roads have recently been paved after being dug up for the installation of new sewer pipes.

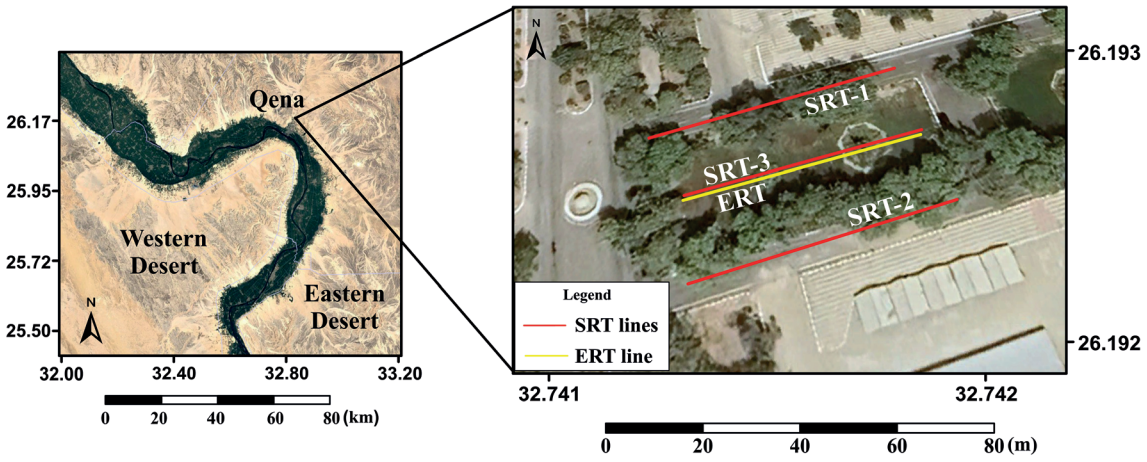

Fig. 1 - Location map of the study area shows the location of the seismic refraction and electrical resistivity acquisition lines, within the South Valley University Campus, east of Qena city.

The information from the nearby boreholes shows that the shallow soil consists of a surface weathered layer of clayey sand and fine to medium sand (Fig. 2). This surface layer has a thickness of 3-6 m. The second layer is the Qena formation, which consists of sands and gravels, and is changed laterally into clay and clayey sand with a thickness of 12-19 m. These layers represent the Quaternary sediments that characterise the shallow subsurface in the Qena area (see: Said, 1971, 1975; Wendorf and Schild, 1976; Askalany, 1988; Issawi and McCauley, 1992; Ibrahim, 2012; Philobbos *et al.*, 2015; Ibrahim *et al.*, 2017).

In August 2022, the northern road subsided, and the southern road collapsed in some areas, creating pits of varying sizes (Fig. 3). The pits ranged in width from a few centimetres to 2 m and have depths from a few centimetres to 1.5 m. The pits were later filled with soft clay and silt, but the problem worsened, and new pits and subsidence formed. The causes of the problem were initially attributed to water from the garden due to constant irrigation. It was suspected that the water from the garden had penetrated the underground shallow layer beneath the asphalt and

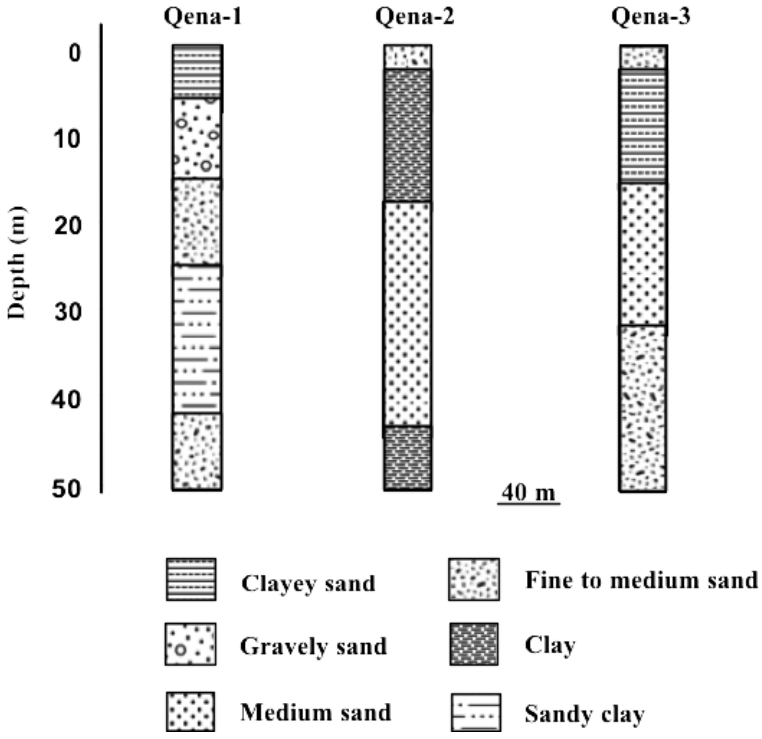

Fig. 2 - Lithological units from three boreholes drilled within South Valley University Campus. These wells are located in agricultural farms and information from well Qena 2 was used for the data interpretation of both ERT and SRT methods as it is the closest to the area under investigation.

Fig. 3 - Images show the pits opened in the asphalt roads, as a result of collapses in the subsoil.

weakened the soil, leading to the collapse of the asphalt road. The main objective of this study is to investigate the cause of the collapse and subsidence of the road. The SRT and ERT methods were used to achieve this goal. The SRT is measured to investigate the soil conditions under the asphalt pavements and in a nearby garden, while the ERT investigates the shallow soil within the garden.

2. Materials and methods

2.1. Seismic refraction tomography (SRT)

SRT is a geophysical technique for mapping subsurface structures depending on the velocity distribution of compressional waves and also shear waves in the subsurface. It enables reconstructing an image of the subsurface distribution of seismic wave velocity and its anomalies with high resolution. SRT involves the creation of an initial synthetic model of the subsurface and, then, determines the smallest deviation between the measurements acquired on the surface and measurements calculated for the synthetic model through an iterative process. The method has proven its effectiveness in shallow target investigations and engineering applications. This includes mapping the bedrock surface, estimating the water table depth, mapping faults and fractures, determining the thickness of unconsolidated sediments, and site characterisation for engineering projects (Redpath, 1973; Belfer *et al.*, 1998; Zhigulev and Patrikeev, 2007; Azwin *et al.*, 2013; Brixová *et al.*, 2018; Umor *et al.*, 2019).

Seismic refraction has frequently been used for pavement characterisation (e.g. Phelps and Cantor, 1966; Amin, 1993; Paine, 1999; Hayashi and Takahashi, 2001). In pavement systems, the stiffness of the very thin upper asphalt layer is usually higher than the stiffness of the base layer. As a result, the P-wave velocity generally decreases with depth, since the velocity of the asphalt concrete layer is usually higher than the base layer (Amin, 1993). This results in the asphalt having a higher velocity than that of the underlying layers. This is called velocity inversion, which constitutes a serious limitation in the seismic refraction interpretation (Nunn and Boztas, 1977; Whiteley and Greenhalgh, 1979). In this context, the response from the asphalt would mask that of the underlying low velocity layer, as, according to Snell's law, no critical refraction at the top of the low velocity layer is possible (Dobrin, 1976; Patskan and Quesada, 2006). Nevertheless, the measured data of this research showed a clear refraction response, which enables a full analysis of the acquired shot records.

Seismic measurements on pavements are sometimes tedious due to the difficulty of coupling the geophones on the rigid asphalt surface. Nevertheless, refraction data can be acquired with sources and receivers either on road shoulders or directly on the pavement. In this case, the seismic refraction method is used to calculate physical properties of the fill, soil, and bedrock beneath the pavement, as well as estimating the depth to the bedrock (e.g. Amin, 1993; Paine, 1999).

In this research, the P-wave refraction data were collected along three parallel acquisition lines oriented in NE-SW direction. Seismic refraction lines SRT-1 and SRT-2 are measured directly on the asphalt roads, while line SRT-3 is measured within the garden and coincides with the ERT line. The total length of each line is 42 m, and each consists of two overlapping spreads. The length of each spread is 24 m with an overlap distance of 6 m. Vertical geophones with a resonant frequency of 14 Hz are used for the acquisition, with a total number of 42 geophones in each line. Due to the small size of the pits, a geophone spacing of 1 m is set for the survey to

ensure the desired lateral resolution. For successful acquisition on asphalt road, the geophones are firmly anchored in specially designed cement blocks, which are placed on the asphalt at the receiver locations for the SRT-1 and SRT-2 lines (Fig. 4). These designed bases were used because it is difficult to fully embed the geophones in the rigid asphalt surface of the road (Rucker, 2003; Moura and Senos Matias, 2012; Shaaban *et al.*, 2013; Liu *et al.*, 2018). Twenty six inline shots with a spacing of 2 m are employed for each acquisition spread, with a distance of 0.5 m between the first shot and the first geophone. A 10-kilogramme sledgehammer is used as a seismic source and the shots are stacked 3 to 5 times. The data are recorded with a 12-channel Geomtrics ES-3000, with a sampling interval of 0.25 ms and a recording length of 200 ms. No acquisition filters are applied.

Fig. 4 - Images show the acquisition of the SRT and ERT data. The upper image shows the acquisition of the seismic data on the asphalt road, where the geophones are inserted on concrete blocks. The lower image shows ERT line acquisition within the garden. The geology and geophysics students of the faculty of sciences assisted in the acquisition process.

2.2. The 2D resistivity imaging

The geoelectrical resistivity method allows investigating the resistivity distribution of rocks and/or soils in the subsurface. The procedure entails injecting an electrical current into the subsurface via a pair of electrodes (C1 and C2) and measuring the potential difference (V) across a pair of electrodes (P1 and P2). The ERT is used to characterise soils (e.g. Sudha *et al.*, 2009) and as a tool in the geotechnical investigation of the substrate of road embankments (e.g. Kowalczyk *et al.*, 2017; Saha and Dey, 2023).

In the geoelectrical survey, resistivities are measured along one line (ERT) of 142.5 m long, coinciding with line SRT-3 in the garden area (Fig. 1). The data along this line were collected using the Terrameter SAS-300C. In this case, we manually applied a multi-electrode configuration with a unit electrode spacing of 1 m. The Wenner array is employed. To achieve the 2D resistivity imagining with Wenner electrode array, 49 electrodes were used with a minimum electrode spacing of 1 m and the total number of data levels was 10 levels. The minimum and maximum values of the measured apparent resistivity are 21.87 Ωm and 92.24 Ωm, respectively.

The SRT and ERT acquisition lines within the garden are measured to investigate whether the water from the irrigation is a cause of the subsidence and collapses in the asphalt road.

2.3. Data analysis

For all seismic data acquired, the geometry, including the coordinates and heights of the shots and geophones, is assigned to the recordings. The first arrival times for the shot records are picked manually using Pickwin, the picking module of the SeisImager software package. For the two lines SRT-1 and SRT-2, where the data were collected on the asphalt road, noise levels in the recordings are relatively high due to road traffic and poor coupling between the ground and geophones. Nevertheless, the data quality is sufficient for manually picking the first arrivals in all data sets. In the shot records, the direct wave in the asphalt was apparent at a very low energy, with a velocity more than that of the subsoil. However, the later-arriving direct and refracted waves from the subsoils were clearly visible on the seismic record and not obscured by the higher velocity asphalt layer (Fig. 5). In this case, picking of the first arrivals would produce a

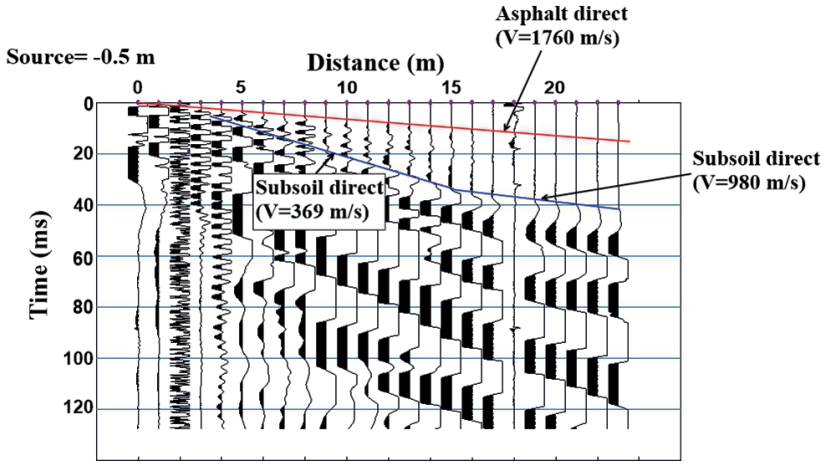

Fig. 5 - A record of the shot at -0.5 m of the line SRT-2 illustrates the clear and observed arrivals from the subsoil layer, as they are not masked by the higher velocity upper asphalt layer.

time skip in the travel time curve (Fig. 6), as the relatively high frequency energy travelling in the high velocity upper layer may fade out before the low frequency arrivals from the lower layer (Whiteley and Greenhalgh, 1979). There are 144 first breaks that are picked from the shot records, and, then, used for the travel time tomography. Examples of selected picked raw shot records are shown in Fig. 7.

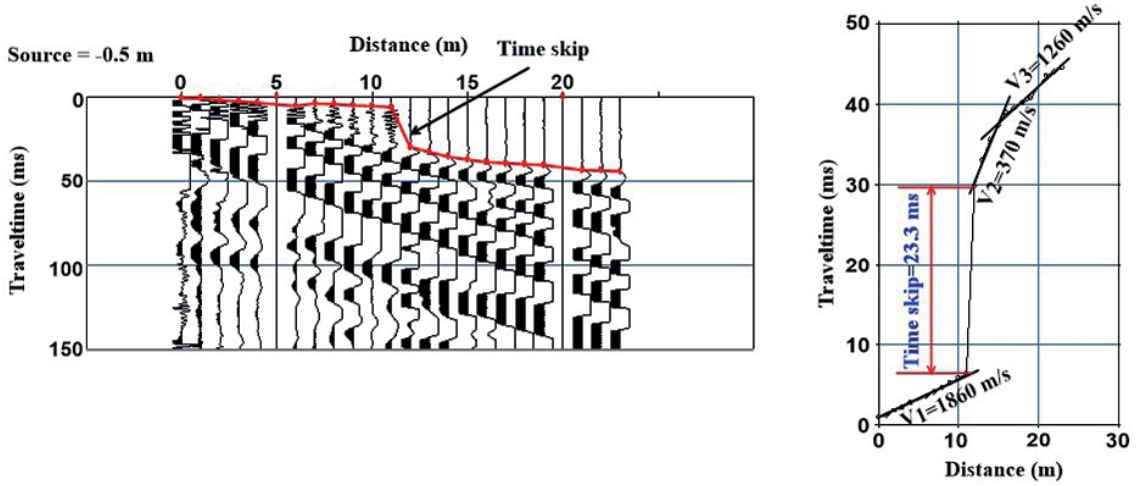

Fig. 6 - An example of shot record from Line SRT-1 shows the time delays produced in the first arrivals due to the presence of the high velocity asphalt above a lower velocity layer.

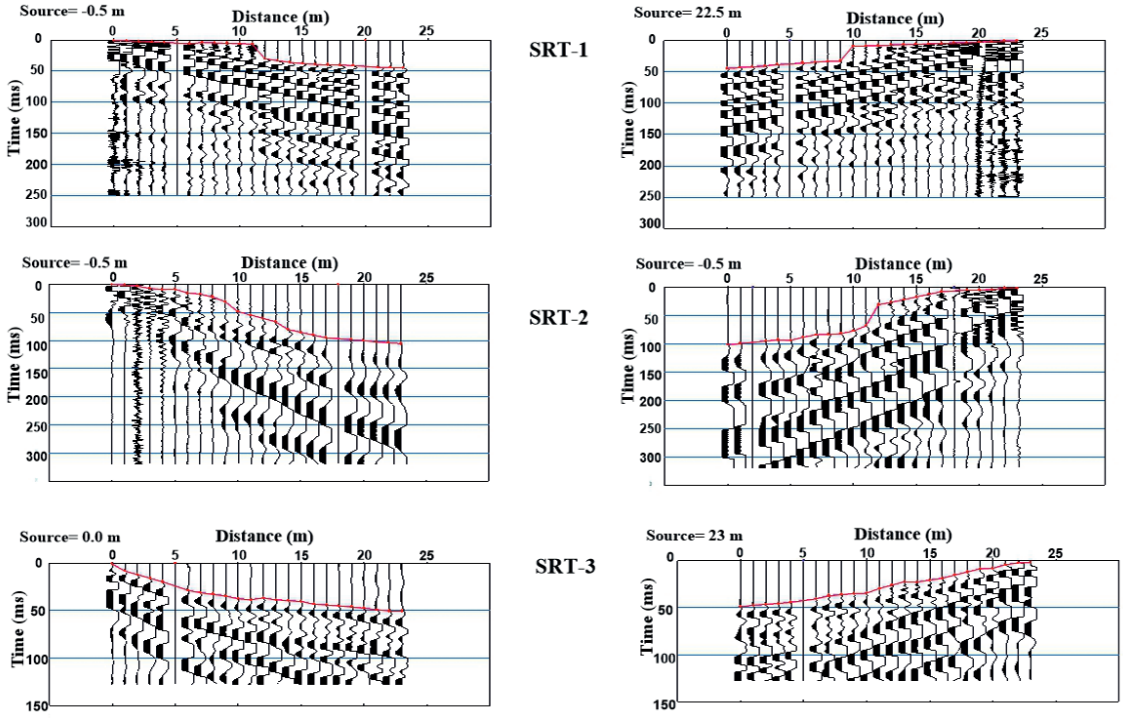

Fig. 7 - Examples of field shot records, showing the picked first arrivals used for the data analysis.

The first breaks are entered into Plotrefa, the SeisImager module used to generate 2D tomograms of the subsurface seismic velocity structure. It uses nonlinear traveltime tomography (Gebrande and Miller, 1985; Rühl, 1995; Zang and Toksöz, 1998) consisting of ray tracing for forward modelling and simultaneous iterative reconstruction technique for inversion. The first arrival times are plotted against source-to-geophone distances, and traveltime-distance curves are estimated and checked for precise interpretation of the data. The initial model is created based on the data from the nearby boreholes.

All the acquired shots are used in the tomographic modeling. The observed and calculated data show a difference in root-mean-square (RMS) error from 1 to 2 m, indicating a good fit between the observed and calculated traveltimes (Fig. 8). Three 2D depth-velocity models are generated by tomographic inversion and are shown in Fig. 8.

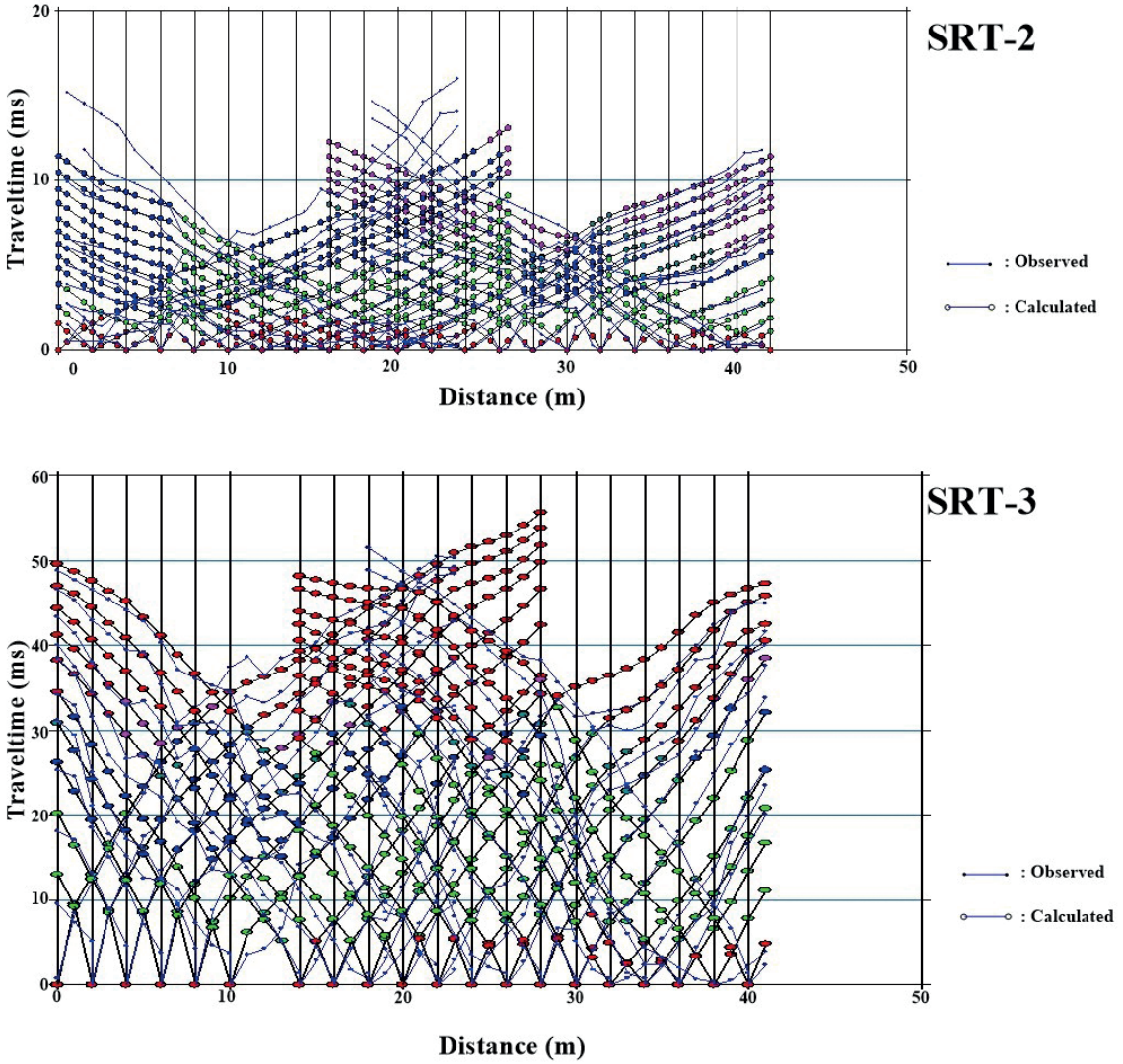

Fig. 8: - Two examples of the observed and calculated traveltimes after the tomographic inversion of SRT-2 and SRT-3 lines. This shows an RMS error of 1.2 m.

The Res2Dinv program (Loke and Barker, 1996) was utilised to process the measured apparent resistivity data. From the inverted resistivity section, we found that the resistivity varies between a minimum value of 23 Ωm to a maximum value of 135 Ωm. The estimated RMS error is 5.4% after five inversion iterations.

3. Results and discussion

The seismic refraction results show a close correlation with the lithological data from well Qena-2 (Fig. 2), which is drilled in an agricultural farm very near to the investigated area. The tomographic models of the lines SRT-1 and SRT-2 (Fig. 9), which were measured on the asphalt roads, show higher velocities compared to the line SRT-3 within the garden. Due to the very thin thickness of the asphalt concrete compared to the underlying filling, as observed in the open pits, the seismic waves would likely manage to penetrate further below the asphalt, particularly when it is underlain by uncompacted soil. In this case and according to Snell's law (Dobrin, 1976), the tomographic inversion routine would not be able to resolve for the abrupt decrease in the velocity from high to very low, as no critical refraction would occur at the asphalt layer. Instead, the resulting models show the general variation of the velocity with higher values than the actual velocities characterising the shallow layers. In this case, the P-wave velocities in the resulting models for these two lines will not express the real velocities of the subsurface shallow layers and only the velocities calculated from the line SRT-3 inside the garden will be considered. When examining SRT-1 and SRT-2 lines, the velocity gradient would be the main parameter for characterising the layers.

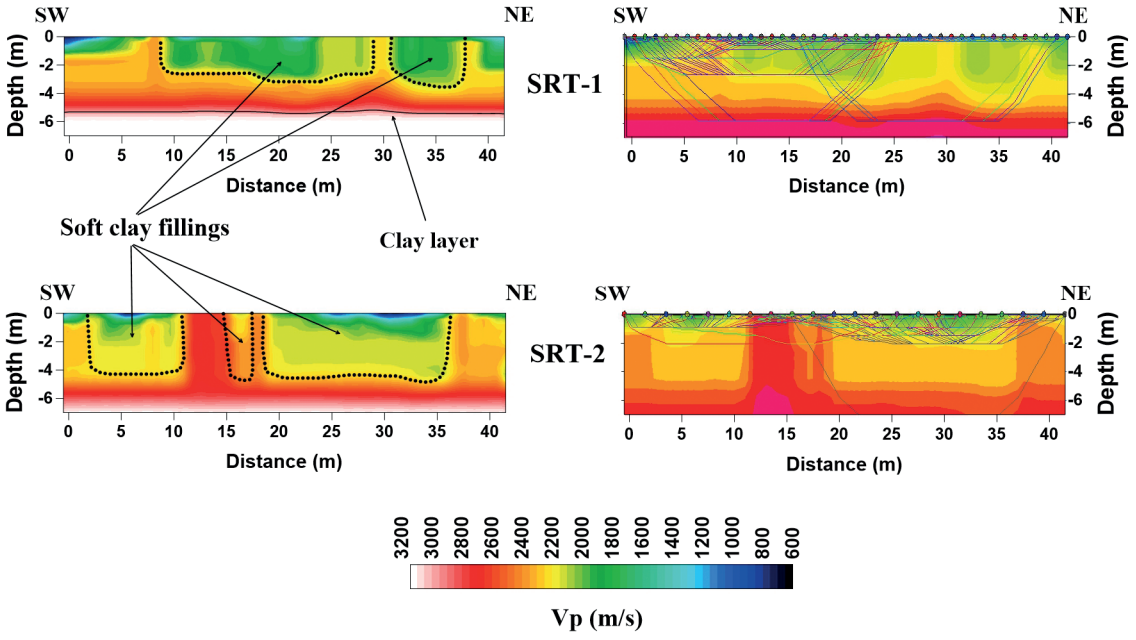

Fig. 9 - The depth-velocity models resulting from the tomographic inversion of the two seismic refraction lines SRT-1 and SRT-2 located at the two asphalt roads. The models are accompanied by ray density coverage. Low velocity anomalies, which represent the soft filling below the thin asphalt layer in the two models, are marked by dotted lines.

In SRT-1 line, two layers were revealed, where the upper layer represents the composite layer of the pavement, while the lower layer consists of clay, as derived from the nearby agricultural farm's Qena-2 well. SRT-2 line shows only the composite layer of the pavement. In the models, the pavement layer is characterised by a low velocity gradient that increases downwards. The clay layer in the SRT-1 line shows a high velocity gradient.

A low velocity anomaly is observed in line SRT-1 at the distance between 9 and 28 m, coinciding with the subsided part of the northern asphalt road. The anomaly extends from the surface to a depth of approximately 3 m. Another anomaly of smaller extent is observed between 30 and 37 m and reaches a maximum depth of about 3.6 m. The lower clay layer is estimated at a depth of 5 m.

In line SRT-2, three distinct low-velocity anomalies are also observed in the upper layer. The first anomaly extends from the beginning of the line to 11.5 m, with a depth of approximately 4 m. The second anomaly with an elongated, narrow shape is observed in the centre of the model at a distance between 14 and 18 m and reaches a depth of about 4.5 m. The third anomaly is observed at a distance of between 19 and 36 m and reaches a depth of approximately 4.5 m. All the anomalies observed in this line coincide with the pits located on the southern asphalt road. As observed in the two models for the asphalt roads, these low velocity anomalies are confined to the upper surface layer, which is the pavement composite layer composed of the very thin asphalt concrete and asphalt base followed by a sub-base layer. The whole pavement has a thickness of about 3 to 5 m.

In the raytracing of the models for SRT-1 and SRT-2 lines, the areas in which the anomalies were observed are bypassed by most of the rays. This behaviour of the seismic rays as well as the velocity drop observed in these areas, indicates fine sand, silt, and soft clay fillings. These soft fillings are observed in-site from the open pits at the surface.

The results of SRT and ERT within the garden are compared and integrated to create a comprehensive image of the soil properties, and their reliability is verified using data from nearby borehole Qena-2.

In the tomographic model of SRT-3 line within the garden, two geoseismic layers are detected (Fig. 10a). The upper surface layer has a P-wave velocity of less than 400 m/s, indicating the fine sand and soft clay soil. The layer has a variable thickness, where it is less than 1 m thin at the distance between 10 and 20 m as well as the distance between 31 and 36 m. The thickness increases to approximately 3 m in the middle of the line. The lower geoseismic layer has a velocity of more than 400 m/s and represents the underlaying clay layer. Unlike the seismic lines on the asphalt road, no anomalies were observed in this line.

Considering the results of the inversion of the apparent resistivity data along the line within the garden, there are two geoelectric layers revealed in the inverted resistivity model (Fig. 10b). The upper geoelectric layer has rather high resistivity values ranging from 40 to 135 Ωm, and a relatively lesser thickness ranging from 0.5 to 2 m, which corresponds to wet fine sand and clay soil. Lower resistivity values ranging from 23 to 39 Ωm characterise the lower geoelectric layer, which may correspond to clay layer. The low electrical resistivity values of less than 100 Ωm are characteristic of the clay layers (Aziz *et al.*, 2013; Burger *et al.*, 2023). These results are in good agreement with those of the SRT-3 inversion. The electrical resistivity and seismic velocity of sand and gravel deposits depend strongly on the moisture content of the materials. Wet sand and gravel deposits have a much lower resistivity, which can be further influenced by salinity, and the seismic velocity is likely to be higher (Wightman *et al.*, 2004). In this case, the velocity of the upper wet sand and gravel is lower than 400 m/s, as it forms the upper loose, weathered, less compact surface layer. The underlying clay is lower in resistivity and has relatively higher velocity of more than 400 m/s.

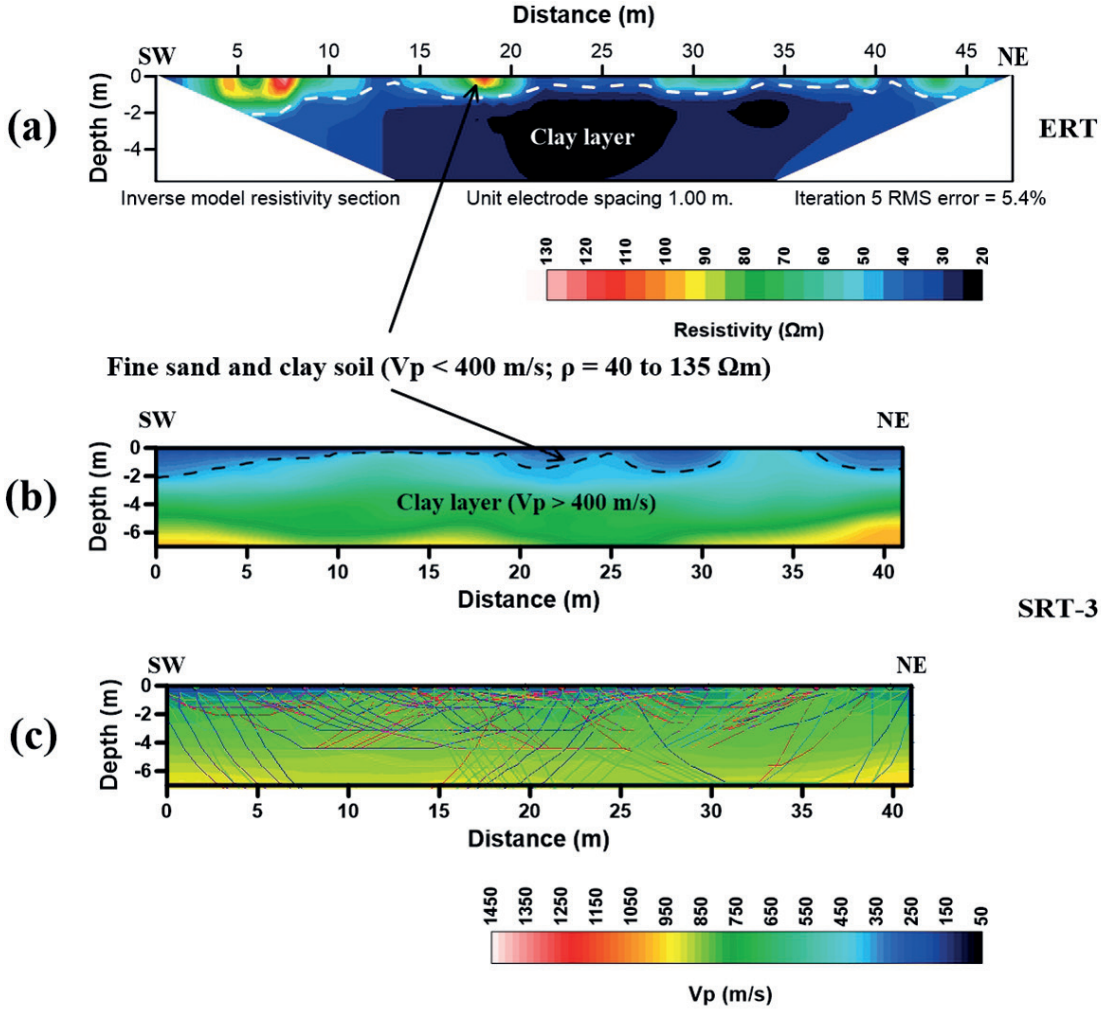

Fig. 10 - a) The electric resistivity 2D model produced by tomographic inversion; b) the seismic refraction tomographic model of line SRT-3, and c) ray density coverage of line SRT-3. The seismic refraction line SRT-3 coincides with the ERT line, and both were acquired within the garden.

4. Conclusions

Seismic refraction tomography and electrical resistivity measurements were used to investigate the causes of the failure of two asphalt roads on the campus of South Valley University, Qena, southern Egypt. The two asphalt roads were affected by subsidence and collapse, forming pits of different sizes. The two roads surround a rectangular garden where irrigation water was suspected to be the cause of the damage. The SRT lines measured on the asphalt roads showed low velocity anomalies consistent with the pits and subsidence sites. The results of the SRT and ERT lines measured within the garden show two layers. The upper layer is wet fine sand and clay soil with a low resistivity of 40-139 Ωm and a P-wave velocity of less than 400 m/s and a thickness of 0.5 to 3 m. The lower layer is characterised by lower resistivities of 29-39 Ωm and a velocity of more than 400 m/s, which could correspond to the clay layer, as can be seen from the lithological information of a nearby well.

It was assumed that the damage to the asphalt road was caused by the garden's irrigation water. However, on-site observations indicate that the water played no part in the damage to either road. The sprinkler irrigation system used to water the garden does not produce the amount of water sufficient to seep into the roads and cause such damage. In addition, we did not observe any seepage of water into the roads or open pits. The soil exposed in the pits is dry. The results of the ERT survey in the garden show that the top layer is wet, which is a normal situation due to irrigation, but not so saturated that the water could seep into the surrounding area.

We determined that the damage to the road occurred after some time of the laying of sewage pipes under the road and at the same time as irrigation started in the garden. The water from the irrigation system takes a very long time to accumulate in the upper layer of soil and saturate it sufficiently to seep into the surrounding area and affect the sub-base layer of the asphalt road. In this context, water is not considered to be the cause of the damage to the asphalt road.

The tomographic inversion of the two SRT lines on the asphalt road show low velocity anomalies confined to the upper layer. These anomalies are characterised by very low velocity gradient and are indications of the presence of weakness zones (Abidin *et al.*, 2012). They represent pockets of soft clay and silt used as fill material for older pits in the road, occupying most of the asphalt's subbase layer. Pockets of soft clay can cause settlement at their locations in the pavement layers (Saha and Dey, 2023). The presence of high proportions of silt and clay reduces the bulk density of the soil and, thus, the compaction (DeJong-Hughes *et al.*, 2001; Askin and Özdemir, 2003). Furthermore, we did not observe gravel in the open pits, which should be added to the soil in such cases to increase the compaction of the soil. These observations indicate that the thin asphalt layer was applied directly to the top weathered layer in the area, which is loose and not compacted enough to meet asphalt paving standards.

We recommend removing the loose soil under the asphalt and replacing it with a compacted base layer that can maintain the road.

Acknowledgments. We would like to thank the president of South Valley University for allowing to acquire the data used in this work. We would also like to thank the students of the Department of Geology, South Valley University, for participating in the data acquisition.

REFERENCES

Abidin M.H.Z., Saad R., Ahmad F., Wijeyesekera D.C. and Baharuddin M.F.T.; 2011: *Application of Geophysical Methods in Civil Engineering*. In: Proc. Malaysian Technical Universities International Conference on Engineering & Technology (MUiCET 2011), Batu Pahat, Malaysia, 12 pp.

Abidin M.H.Z., Saad R., Ahmad F., Wijeyesekera D.C. and Baharuddin M.F.T.; 2012: *Seismic refraction investigation on near surface landslides at the Kundasang area in Sabah, Malaysia*. Procedia Eng., 50, 516-531, doi: 10.1016/j.proeng.2012.10.057.

Aizebeokhai A., Oni A. and Oyeyemi K.; 2018: *Groundwater exploration in crystalline basement complex using seismic refraction and electrical resistivity tomography: case study of Olomore, Abeokuta, southwestern Nigeria.* In: Abstract AGU, Fall Meeting 2018, Washington, DC, USA, 2 pp.

Amin M.S.; 1993: *Application of seismic refraction techniques in engineering practice with special emphasis on pavement systems*. Arizona State University, Tempe, AZ, USA, 544 pp.

Araffa S.A.S., Atya M.A., Mohamed A.M.E., Gabala M., Zaher M.A., Soliman M.M., Mesbah H.S., Massoud U. and Shaaban H.M.; 2014: *Subsurface investigation on Quarter 27 of May 15th city, Cairo, Egypt using electrical resistivity tomography and shallow seismic refraction techniques*. NRIAG J. Astron. Geophys., 3, 170-183, doi: 10.1016/j.nrjag.2014.10.004.

Araffa S.A.S., Mohamed A.M.E. and Santos F.M.; 2017: *Geophysical investigation in the northwestern part of the Gulf of Suez, Egypt.* Egypt. J. Pet., 26, 457-475, doi: 10.1016/j.ejpe.2016.06.002.

Araffa S.A.S., Soliman S.A., El Khafif A., Younis A. and Shazley T.F.; 2019: *Environmental investigation using geophysical data at East Sadat City, Egypt*. Egypt. J. Pet., 28, 117-125, doi: 10.1016/j.ejpe.2018.12.002.

Askalany M.M.S.; 1988: *Geological studies on the Neogene and Quaternary sediments of the Nile Basin, Upper Egypt*. PH.D. Thesis in Geological Sciences, Assiut University, Assiut, Egypt, 254 pp.

Askin T. and Özdemir N.; 2003: *Soil bulk density as related to soil particle size distribution and organic matter content*. Poljoprivreda, 9, 52-55.

Aziz N.A., AL- Qaissy M.R. and Karim H.H.; 2013: *Differentiating clayey soil layers from Electrical Resistivity Imaging (ERI) and Induced Polarization (IP)*. Eng. Technol. J., 31, 3216-3234, doi: 10.30684/etj.31.17A.1.

Azwin I.N., Saad R. and Nordiana M.; 2013: *Applying the seismic refraction tomography for site characterization.* APCBEE Procedia, 5, 227-231, doi: 10.1016/j.apcbee.2013.05.039.

Azwin I.N., Saad R., Saidin M., Nordiana M.M., Bery A.A. and Hidayah I.N.E.; 2015: *Combined analysis of 2-D electrical resistivity, seismic refraction and geotechnical investigations for Bukit Bunuh complex crater*. IOP Conf. Ser.: Earth Environ. Sci., 23, 012013, 6 pp., doi: 10.1088/1755-1315/23/1/012013.

Belfer I., Bruner I., Keydar S., Kravtsov A. and Landa E.; 1998: *Detection of shallow objects using refracted and diffracted seismic waves.* J. Appl. Geophys., 38, 155-168, doi: 10.1016/S0926-9851(97)00025-6.

Brixová B., Mosná A. and Putiška R.; 2018: *Applications of shallow seismic refraction measurements in the western Carpathians (Slovakia): case studies*. Contrib. Geophys. Geod., 48, 1-21, doi: 10.2478/congeo-2018-0001.

Burger H.R., Sheehan A.F. and Jones C.H.; 2023: *Introduction to Applied Geophysics*: *exploring the shallow subsurface*. Cambridge University Press, Cambridge, UK, 622 pp., doi: 10.1017/9781009433112.

Butchibabu B., Khan P.K. and Jha P.C.; 2019: *Foundation evaluation of underground metro rail station using geophysical and geotechnical investigations*. Eng. Geol., 248, 140-154, doi: 10.1016/j.enggeo.2018.12.001.

Cardarelli E., Cercato M. and De Donno G.; 2014: *Characterization of an earth-filled dam through the combined use of electrical resistivity tomography, P- and SH-wave seismic tomography and surface wave data*. J. Appl. Geophys., 106, 87-95, doi: 10.1016/j.jappgeo.2014.04.007.

De Nardis R., Cardarelli E. and Dobroka M.; 2005: *Quasi-2D hybrid joint inversion of seismic and geoelectric data*. Geophys. Prospect., 53, 705-716, doi: 10.1111/j.1365-2478.2005.00497.x.

de Pasquale G., Linde N. and Greenwood A.; 2019: *Joint probabilistic inversion of DC resistivity and seismic refraction data applied to bedrock/regolith interface delineation*. J. Appl. Geophys., 170, 103839, 37 pp., doi: 10.1016/J.JAPPGEO.2019.103839.

DeJong-Hughes J.M., Swan J.B., Moncrief J.F. and Voorhees W.B.; 2001: *Soil compaction: causes, effects and control.* University of Minnesota, St. Paul, MN, USA, FO-3115-S, 15 pp.

Demirci İ., Candansayar M.E., Vafidis A. and Soupios P.; 2017: *Two dimensional joint inversion of direct current resistivity, radio-magnetotelluric and seismic refraction data: an application from Bafra Plain, Turkey*. J. Appl. Geophys., 139, 316-330, doi: 10.1016/J.JAPPGEO.2017.03.002.

Dobrin M.B.; 1976: *Introduction to geophysical prospecting, 3rd ed.* McGraw-Hill Pub. Co., New York, NY, USA, pp. 25-56, 292-336, 568-620.

Fernández-Baniela F., Arias D. and Rubio-Ordóñez Á.; 2021: *Seismic refraction and electrical resistivity tomographies for geotechnical site characterization of two water reservoirs (El Hierro, Spain)*. Near Surf. Geophys., 19, 199-223, doi: 10.1002/nsg.12152.

Gallardo L.A. and Meju M.A.; 2003: *Characterization of heterogeneous near-surface materials by joint 2D inversion of DC resistivity and seismic data*. Geophys. Res. Lett., 30, 1658, 4 pp., doi: 10.1029/2003GL017370.

Gallardo L.A. and Meju M.A.; 2004: *Joint two-dimensional DC resistivity and seismic travel time inversion with cross-gradients constraints*. J. Geophys. Res.: Solid Earth, 109, B03311, 11 pp., doi: 10.1029/2003JB002716.

Garofalo F., Sauvin G., Socco L.V. and Lecomte I.; 2015: *Joint inversion of seismic and electric data applied to 2D media*. Geophys., 80, EN93-EN104, doi: 10.1190/geo2014-0313.1.

Gebrande H. and Miller H.; 1985: *Refraktionsseismik*. In: Bender F. (ed), Angewandte Geowissenschaften Band II, Methoden der Angewandten Geophysik und Mathematische Verfahren in Geowissenschaften, F. Enke Verlag, Stuttgart, Germany, pp. 226-260.

Gunther T. and Rucker C.; 2006: *A new joint inversion approach applied to the combined tomography of DC resistivity and seismic refraction data*. In: Extended Abstract, 19th Environment and Engineering Geophysical Society Annual Meeting, Symposium on the Application of Geophysics to Engineering and Environmental Problems, Seattle, WA, USA, pp. 1196-1202, doi: 10.4133/1.2923578.

Hayashi K. and Takahashi T.; 2001: *High resolution seismic refraction method using surface and borehole data for site characterization of rocks*. Int. J. Rock Mech. Min. Sci., 38, 807-813, doi: 10.1016/S1365-1609(01)00045-4.

Ibrahim A.M.; 2012: *Geotechnical and sedimentological studies of the Quaternary sediments at Qena Region, Egypt*. In: Proc. Geology of the Nile Basin Countries Conference (GNBCC-2012), Alexandria, Egypt.

Ibrahim A.M., Cesarano M., Calcaterra D., Cappelletti P., Graziano F., Ramondini M. and Mansour A.M.; 2017: *Preliminary results of the strength characteristics of Pliocene Durri formation exposed along Qena-Safaga road, Egypt*. In: Proc. 9th International Conference on the Geology of Africa, Assiut, Egypt, p. 76.

Imani P., Tian G., Hadiloo S. and El-Raouf A.A.; 2021: *Application of combined electrical resistivity tomography (ERT) and seismic refraction tomography (SRT) methods to investigate Xiaoshan District landslide site: Hangzhou, China*. J. Appl. Geophys., 184, 104236, 13 pp., doi: 10.1016/j.jappgeo.2020.104236.

Issawi B. and McCauley J.F.; 1992: *The Cenozoic Rivers of Egypt: the Nile problem*. In: Freidman R. and Adams B. (eds), The Followers of Horus, Oxford Press, Oxford, UK, pp. 121-138.

Kowalczyk S., Piotr Z. and Maciej M.; 2017: *Application of the electrical resistivity method in assessing soil for the foundation of bridge structures: a case study from the Warsaw environs, Poland*. Acta Geodyn. Geomater., 14, 221-234, doi: 10.13168/AGG.2017.0005.

Liu P., Wang D., Otto F., Hu J. and Oeser M.; 2018: *Application of semi-analytical finite element method to evaluate asphalt pavement bearing capacity*. Int. J. Pavement Eng., 19, 479-488, doi: 10.1080/10298436.2016.1175562.

Loke M.H. and Barker R.D.; 1996: *Rapid least-squares inversion of apparent resistivity pseudosections by a quasi-Newton method*. Geophys. Prospect., 44, 131-152, doi: 10.1111/j.1365-2478.1996.tb00142.x.

Moura R.M. and Senos Matias M.J.; 2012: *Geophones on blocks: a prototype towable geophone system for shallow land seismic investigations*. Geophys. Prospect., 60, 192-200, doi: 10.1111/j.1365-2478.2011.00963.x.

Nunn K.R. and Boztas M.; 1977: *Shallow seismic reflection profiling on land using a controlled source*. Geoexplor., 15, 87-97, doi: 10.1016/0016-7142(77)90015-1.

Paine J.G.; 1999: *Using geologic maps and seismic refraction in pavement-deflection analysis.* Research and Technology Transfer Section, Center for Transportation Research, Dept. Transportation, University of Texas, Austin, TX, USA, Tech. report, TX-00/2990-S, 127 pp.

Patskan J. and Quesada R.M.; 2006: *Seismic refraction response on an asphalt covered surface*. In: Proc. 19th Symposium on the Application of Geophysics to Engineering and Environmental Problems, SAGEEP 2006, Environment and Engineering Geophysical Society, Seattle, WA, USA, pp. 1027-1033, doi: 10.4133/1.2923560.

Pavoni M., Boaga J., Wagner F.M., Bast A. and Phillips M.; 2023: *Characterization of rock glaciers environments combining structurally-coupled and petrophysically-coupled joint inversions of electrical resistivity and seismic refraction datasets*. J. Appl. Geophys., 215, 105097, 18 pp., doi: 10.1016/j.jappgeo.2023.105097.

Phelps J.M. and Cantor T.R.; 1966: *Detection of concrete deterioration under asphalt overlays by microseismic refraction*. Highway Res. Rec., 146, 34-49.

Philobbos E.R., Essa M.A. and Ismail M.M.; 2015: *Geologic history of the Neogene "Qena Lake" developed during the evolution of the Nile Valle*y: *a sedimentological, mineralogical and geochemical approach*. J. Afr. Earth Sci., 101, 194-219, doi: 10.1016/j.jafrearsci.2014.09.006.

Qaher M., Eldosouky A.M., Saada S.A. and Basheer A.A.; 2023: *Integration of ERT and shallow seismic refraction for geotechnical investigation on El-Alamein Hotel Building area, El-Alamein new city, Egypt.* Geomech. Geophys. Geo-energ. Geo-resour., 9, 115, 23 pp., doi: 10.1007/s40948-023-00639-8.

Redpath B.B.; 1973: *Seismic refraction exploration for engineering site investigations*. NTIS, U.S. Department of Commerce, National Technical Information Service, Springfield, VA, USA, Tech. report E-73-4, 63 pp.

Remmani S.A., Madun A. and Kamaruddin N.H.; 2020: *Asphalt pavement thickness measurement using the seismic reflection technique*. Int. J. Sci. Technol. Res., 9, 527-531.

Ronczka M., Hellman K., Günther T., Wisén R. and Dahlin T.; 2017: *Electric resistivity and seismic refraction tomography: a challenging joint underwater survey at Äspö Hard Rock Laboratory*. Solid Earth, 8, 671-682, doi: 10.5194/se-8-671-2017.

Rucker M.L.; 2003: *Applying the refraction microtremor (ReMi) shear wave technique to geotechnical characterization*. In: Proc. 3rd International Conference on the Application of Geophysical Methodologies and NDT to Transportation and Infrastructure, Orlando, FL, USA, pp. 8-12.

Rühl T.; 1995: *Determination of shallow refractor properties by 3D CMP refraction seismic techniques*. First Break, 13, 69-77, doi: 10.3997/1365-2397.1995005.

Saha A. and Dey A.K.; 2023: *Assessing combined analysis of electrical resistivity tomography and multichannel analysis of surface waves for ground improvement assessment near by-pass road, Silchar, Assam*. Explor. Geophys., 54, 474-492, doi: 10.1080/08123985.2023.2168533.

Said R.; 1971: *Explanatory notes to accompany the geological map of Egypt.* Geological Survey of Egypt, 3, 89-105.

Said R.; 1975: *The geological evolution of the River Nile*. In: Wendorf F. and Marks A.E. (eds), Problems in prehistory northern Africa and the Levant, Southern Methodist University Press, Dallas, TX, USA, 144 pp., doi: 10.1007/978-1-4612-5841-4.

Shaaban F., Ismail A., Massoud U., Mesbah H., Lethy A. and Abbas A.M.; 2013: *Geotechnical assessment of ground conditions around a tilted building in Cairo-Egypt using geophysical approaches*. J. Assoc. Arab Univ. Basic Appl. Sci., 13, 63-72, doi: 10.1016/J.JAUBAS.2012.06.002.

Sudha K., Israil M., Mittal S. and Rai J.; 2009: *Soil characterization using electrical resistivity tomography and geotechnical investigations*. J. Appl. Geophys., 67, 74-79, doi: 10.1016/j.jappgeo.2008.09.012.

Umor M.R., Arifin M.H. and Muda N.; 2019: *The seismic refraction survey to determine the depth of bedrock at the Damansara area for horizontal directional drilling method application*. Appl. Sci. Innov. Res., 3, 123, doi: 10.22158/asir.v3n3p123.

Vagnon F., Comina C. and Arato A.; 2022a: *Evaluation of different methods for deriving geotechnical parameters from electric and seismic streamer data*. Eng. Geol., 303, 106670, 25 pp., doi: 10.1016/j.enggeo.2022.106670.

Vagnon F., Comina C., Arato A., Chiappone A., Cosentini R.M. and Foti S.; 2022b: *Geotechnical screening of linear earth structures: electric and seismic streamer data for hydraulic conductivity assessment of the Arignano Earth dam, Italy*. J. Geotech. Geoenviron. Eng., 148, 4022105, 38 pp, doi: 10.1061/(ASCE)GT.1943-5606.0002911.

Villani F., Tulliani V., Sapia V., Fierro E., Civico R. and Pantosti D.; 2015: *Shallow subsurface imaging of the Piano di Pezza active normal fault (central Italy) by high-resolution refraction and electrical resistivity tomography coupled with time-domain electromagnetic data*. Geophys. J. Int., 203, 1482-1494, doi: 10.1093/gji/ggv399.

Wagner F.M., Mollaret C., Günther T., Kemna A. and Hauck C.; 2019: *Quantitative imaging of water, ice and air in permafrost systems through petrophysical joint inversion of seismic refraction and electrical resistivity data.* Geophys. J. Int., 219, 1866-1875, doi: 10.1093/gji/ggz402.

Wendorf F. and Schild R.; 1976: *Prehistory of the Nile Valley*. Academic Press Inc., London, UK, 404 pp.

Whiteley R.J. and Greenhalgh S.A.; 1979: *Velocity inversion and the shallow seismic refraction method*. Geoexplor., 17, 125-141, doi: 10.1016/0016-7142(79)90036-X.

Whitlow R.; 1995: *Basic Soil Mechanics* (*3rd ed*). Longman Group Ltd, Essex, England, 559 pp.

Wightman E., Jalinoos F., Sirles P. and Hanna K.; 2004: *Application of geophysical methods to highway related problems*. Federal Highway Administration, Central Federal Lands Highway Division, West Dakota Avenue, Lakewood, CO, USA, FHWA-IF-04-021, 742 pp.

Yilmaz O., Eser M. and Berilgen M.; 2006: *Seismic, geotechnical, and earthquake engineering site characterization*. In: Expanded Abstracts, SEG Technical Program, Society of Exploration Geophysicists, New Orleans, LA, USA, pp. 1401-1405, doi: 10.1190/1.2369781.

Zakaria M.T., Taib A., Saidin M.M., Saad R., Muztaza N.M. and Masnan S.S.K.; 2018: *Correlation of geophysical and geotechnical methods for sediment mapping in Sungai Batu, Kedah*. J. Phys. Conf. Ser., 995, 12082, 7 pp.

Zang, J. and Toksöz M.N.; 1998: *Nonlinear refraction traveltime tomography*. Geophys., 63, 1726-1737.

Zhigulev V.V. and Patrikeev V.N.; 2007: *Shallow seismic refraction analysis: application to studying the active North Sakhalin fault*. Russ. J. Pac. Geol., 1, 15-21, doi: 10.1134/S1819714007010034.

Corresponding author: Mahmoud Ahmed Abbas
Dipartimento di Scienze della Tera, dell'Ambiente e delle Risorse (DiSTAR)
Università degli Studi di Napoli Federico II
Complesso Universitario di Monte Sant'Angelo
Via Vicinale Cupa Cintia 21, 80126 Napoli, Italy
Phone: +39 081 2538334; e-mail: mahmoud.ahmed1@sci.svu.edu.eg, mahmoud.abbas@unina.it